RSC Advances

PAPER

View Article Online
View Journal | View Issue

Cite this: *RSC Adv.*, 2026, **16**, 17462

Reactions of dissolved organic matter with hydroxyl radicals: effects on DOM molecular properties and modulation by Cu(II)

Zhansheng Li, Hongxia Zhao * and Shafiul Azam

The reaction of hydroxyl radical (˙OH) with dissolved organic matter (DOM) is a key process in engineered and natural aquatic systems. In this study, the second reaction rate constants between ˙OH and three kinds of DOM ($k_{DOM,\cdot OH}$) were measured and the changes of molecular properties of DOM induced by ˙OH were characterized. The room-temperature $k_{DOM,\cdot OH}$ value ranged from 3.26 to 7.38 × 10^9 M_C^{-1} s^{-1}. Oxidation by ˙OH led to mineralization, bleaching of chromophoric groups, and alterations in fluorescent moieties, as revealed by UV-vis and fluorescence spectroscopy. The presence of cupric ion (Cu^{2+}) decreased $k_{DOM,\cdot OH}$ values for all three kinds of DOM to varying extents. The interaction mechanism between DOM and Cu^{2+} indicated the aggregation of the DOM fragment for the cation bridge effect and charge transfer from ligand to metal for the electron shuttle effect of Cu^{2+} were the dominant reasons for the decrease of $k_{DOM,\cdot OH}$. Spectroscopic indices, hydrodynamic size, and XPS analyses indicate that this inhibition is mainly attributable to Cu^{2+}-induced aggregation of DOM *via* cation bridging and coordination with electron-donating functional groups, which reduces the accessibility of reactive sites to ˙OH. In addition, ligand-to-metal charge transfer and the associated Cu(II)/Cu(I) electron-shuttle behavior likely provide a supplementary pathway that further suppresses DOM oxidation. Overall, these results show that DOM significantly reduces the effective utilization of ˙OH in advanced oxidation processes and can inhibit ˙OH-driven degradation of organic pollutants, while the observed mineralization and optical changes provide insight into the fate and transformation of DOM in natural and engineered waters.

Received 4th December 2025
Accepted 10th February 2026

DOI: 10.1039/d5ra09373b

rsc.li/rsc-advances

1. Introduction

Dissolved organic matter (DOM) is an important participant of photochemical processes in aquatic environments.[1,2] Besides the sources of photochemically produced reactive intermediates (PPRIs), such as hydroxyl radical (˙OH), singlet oxygen ($^1O_2$), and triplet excited state of DOM (^{3}DOM*),[1,3,4] DOM can also serve as a sink for these PPRIs, especially for ˙OH.[5,6] The reductant moiety of DOM (phenols, aromatic alcohol *etc.*) competitively quenches these PPRIs,[7] leading to photobleaching, oxidation and photo-mineralization of DOM, which subsequently affects the biogeochemical cycling of carbon.[8,9] In addition, the reactivity between DOM and PPRIs can inhibit the indirect photodegradation of organic pollutants induced by PPRIs.[10] Furthermore, due to the widespread use of ˙OH in advanced oxidation and other water treatment processes, the presence of DOM in water can affect the treatment efficiency during the advanced oxidation process by quenching ˙OH.[5] Therefore, it is necessary to investigate the reactivity of DOM with ˙OH to evaluate its role in the degradation of pollutants caused by ˙OH in various environmental processes and in the carbon cycle in aquatic environments.

˙OH is a strong oxidant (+2.8 eV *vs.* SHE) that acts as a non-selective oxidant in water and has very high reactivity towards organic pollutants and organic matter, up to a diffusion rate-controlled rate.[6,11–13] The high reactivity leads to a shorter lifetime in aquatic environments, but due to its wide range of sources, the steady-state concentration in natural water is 10^{-17}–10^{-15} M , and the concentration in advanced oxidation processes can even reach about 10^{-9} M.[5,14,15] ˙OH could oxidize organic matter through hydroxide, hydrogen and electron transfer processes, resulting the bleaching, oxidation and mineralization of DOM.[15] However, there remains a lack of clear insight into the effects of ˙OH on the optical properties of DOM. Previous studies on the reaction between ˙OH and DOM have mainly focused on its impact on the degradation of organic pollutants, whereas the effects on DOM itself have received much less attention.[10] Due to DOM being the main organic carbon reservoir in water bodies, it is necessary to study the changes in DOM molecular properties induced by ˙OH.

The reactivity of DOM toward ˙OH was evaluated by measuring the bimolecular reaction rate constant between DOM and ˙OH ($k_{DOM,\cdot OH}$). $k_{DOM,\cdot OH}$ usually measured using

Key Laboratory of Industrial Ecology and Environmental Engineering (Ministry of Education), School of Environmental Science and Technology, Dalian University of Technology, Linggong Road 2, Dalian 116023, China. E-mail: hxzhao@dlut.edu.cn; Fax: +86(411)-84706552 22; Tel: +86(411)-84706552

laser flash photolysis (LFP) and typically ranges from 10^8 to 10^9 M_C^{-1} s^{-1}, depending on the intrinsic molecular properties of DOM, water chemical components and so on.[6,12,13,16] Fernando's group has conducted preliminary studies on $k_{DOM,^{\cdot}OH}$ of organic pollutants and organic matter with $^{\cdot}OH$.[6,17] However, the reaction rate constant between DOM and $^{\cdot}OH$ is influenced by environmental factors such as temperature, DOM's characteristics (molecular size, electron donating ability, and other properties), and environmental composition.[6,13] However, there remained lack of a clear investigation about the effects of metal cation on $k_{DOM,^{\cdot}OH}$.

Copper ion (Cu^{2+}), as a typical redox active transient metal cation, broadly coexists in aquatic environment with DOM. The formation of Cu-DOM complexes is well known for the abundant of carboxyl phenolic, aromatic ketonic functional groups in DOM. Cu-DOM complexes are expected to affect the reactivity of DOM toward $^{\cdot}OH$, but the mechanisms by which Cu^{2+} influences $k_{DOM,^{\cdot}OH}$ are still unclear. Pan *et al.* found that Cu^{2+} can inhibit the process of DOM photobleaching, and attributed this to the electron transfer process from ligands to metals (LMCT) during light irradiation.[18] The generated Cu^{+} can be an intermediate of DOM in the process of photooxidation, reducing it back to its initial state and thus inhibiting DOM photobleaching. Herein, the impact of Cu^{2+} on $k_{DOM,^{\cdot}OH}$ and potential mechanism were investigated in this study.

Overall, the objective of this study was to investigate the reactivity of DOM to $^{\cdot}OH$ and exploring the potential effects on the molecular properties of DOM. In addition, the effects of Cu^{2+} on $k_{DOM,^{\cdot}OH}$ and the possible influence mechanism of were also exploring. Firstly, LFP was used to quantify the $k_{DOM,^{\cdot}OH}$ of three kinds of DOM in the absence and presence of Cu^{2+}. Secondly, the changes of molecular properties of DOM induced by $^{\cdot}OH$ were characteristic with multiple spectra. Lastly, the potential effect mechanisms of Cu^{2+} on $k_{DOM,^{\cdot}OH}$. were explored through the interaction mechanism between Cu^{2+} and DOM. The results give an insight into environmental behavior of DOM in water and provide a basis for evaluating the environmental behavior and biogeochemical cycling of organic carbon.

2. Materials and method

2.1 Chemicals and sample preparation

Three humic acid samples (an important component of DOM,as represent of DOM) were obtained from Sigma-Aldrich and purified to remove the metal ions prior to use according to our previous studies. The FT-IR and elemental compositions of these samples were shown in Fig. S1 and Table S2. Sodium nitrite ($NaNO_2$), sodium perchlorate ($NaClO_4$), copper perchlorate ($Cu(ClO_4)_2$), perchloric acid ($HClO_4$), sodium hydroxide (NaOH), hydrogen peroxide (H_2O_2) and sodium thiocyanate (NaSCN) were purchased from Alladin Shanghai company. All solutions were prepared using 18.2 MΩ cm^{-1} ultrapure water from a laboratory water purification system.

All solutions were prepared with ultrapure water. 300 mL of 0.83 $mmol_C$ L^{-1} DOM solutions were prepared at pH 7.0 (adjust with NaOH and $HClO_4$), and added 0.1 mM $NaClO_4$ to control ion strength. Cu^{2+} concentrations in final solutions were 0, 0.2, 1 and 20 μM. All solutions were shaken for 24 h in the dark at 25 °C after titration to ensure that Cu^{2+}-DOM complexation reached equilibrium. The changes of different molecular properties induced by Cu^{2+} were shown in SI.

2.2 Laser flash photolysis experiment

In this study, 355 nm laser was used to excite NO_2^- as a source of $^{\cdot}OH$ in water. Add 0.1 mmol L^{-1} $NaNO_2$ to each sample and adjust the pH to 7 using NaOH and $HClO_4$. The mechanism (Mechanism 1) of $^{\cdot}OH$ generation in the experiment system is shown as in the below equations:[19]

$$NO_2^- \xrightarrow{266nm} [NO_2^-]^*$$

$$[NO_2^-]^* \rightarrow NO^{\cdot} + O^{\cdot-}$$

$$O^{\cdot-} + H_2O \rightarrow {}^{\cdot}OH + OH^-$$

The $k_{DOM,^{\cdot}OH}$ values were measured using laser flash photolysis (LFP). Using LFP analysis, samples containing different concentrations of DOM (from 0.14 $mmol_C$ L^{-1} to 0.42 $mmol_C$ L^{-1}) and fixed concentrations of NaSCN were subjected to 4 ns pulse excitation of OH sensitizer (1 mM $NaNO_2^-$) in H_2O at 355 nm, and SCN^- (100 μM) was used as a competitor. By calculating the changes of $(SCN)_2^{\cdot-}$, $k_{DOM,^{\cdot}OH}$ were found to have an absorption peak at 474 nm. $k_{DOM,^{\cdot}OH}$ can be calculated as following equation.

$$\frac{\left[(SCN)_2^{\cdot-}\right]_0}{\left[(SCN)_2^{\cdot-}\right]} = 1 + \frac{k_1[DOM]}{k_2[SCN^-]}$$

Among them, $[(SCN)_2{}^{\cdot-}]_0$ is the transient absorbance at 475 nm when only SCN^- is present in the system. The absorbance of $[(SCN)_2{}^{\cdot-}]$ represent the transient absorbance at 475 nm when both NaSCN and different concentration of DOM are present in the system, which decreases with increasing DOM concentration. Therefore, the relationship graph between $[(SCN)_2{}^{\cdot-}]_0/[(SCN)_2{}^{\cdot-}]$ and concentration ratio [DOM]/[SCN^-] gives a straight line with a slope of k_1/k_2. By using the rate constant $k_2 = 1.05 \times 10^{10}$ M^{-1} s^{-1} for the reaction between $^{\cdot}OH$ and SCN^-, the $k_{DOM,^{\cdot}OH}(k_1)$ rate constants can be easily determined.

2.3 Steady state photolysis experiment

The reaction between $^{\cdot}OH$ and DOM generated by irradiating H_2O_2 with ultraviolet light was carried out in the XPA-1 rotary photochemical reactor (Nanjing Xujiang Electromechanical Factory) to illustrate the changes in optical properties of DOM. The light source adopts a 500 W mercury lamp, and short wavelength ultraviolet light is filtered out with a 290 nm filter, the spectra of mercury lamp was shown in Fig. S2. The photochemical reactor is connected to a circulating cooling device to maintain a constant reaction temperature (25 °C). A DOM solution (pH = 7) is prepared and placed in a quartz test tube,

with an initial concentration of 0.83 $mmol_C$ L^{-1}(TOC). The initial concentration of H_2O_2 is 100 mmol L^{-1}, and in order to ensure sufficient and stable concentrations of ·OH throughout the entire reaction process, 100 mmol L^{-1} of H_2O_2 is replenished every 0.5 hours. The volume of H_2O_2 replenished accounts for only 1% of the reaction system volume and will not affect the stability of the reaction system. Samples are taken every 0.5 hours and DOC testing is performed immediately after sampling; The UV-vis absorbance and three-dimensional excited emission matrix (3D-EEM) fluorescence spectra were also measured to explore the changes induced by ·OH and Cu^{2+} in the molecular properties of DOM according to our previous studies. The fluorescence index (FI) was calculated as the ratio of emission intensity at 470 nm to that at 520 nm at fixed excited wavelength of 370 nm. And the humification index was calculated as the ratio of the integration of fluorescence intensity from 435 to 480 nm to that from 300 to 345 nm at fixed excited wavelength of 254 nm. Some absorbance spectra indexes, such as SUVA254, E2/E3, SR were also calculated according to previous study and these data were shown in Table S1.

3. Results and discussion

3.1 Determination of reaction rate constants between DOM and hydroxyl radicals

NO_2^- is one of the important sources of ·OH in natural water, and the absorption spectrum of NO_2^- was shown in SI (Fig. S3). In this experiment, a laser at a wavelength of 355 nm was used to excite NO_2^- as a source of ·OH in water (Scheme 1).[19] Due to the extremely short lifetime of ·OH in water, it is hard to exactly capture ·OH by ns level resolution transient absorption spectra. Therefore, thiocyanate (SCN^-) was used as a capture agent for ·OH, and the formation of ·OH in the system was indirectly observed by measuring the signals of absorbance intensity of $(SCN)_2^{\cdot-}$ generated by ·OH and SCN^- (Fig. 1a).[6,13,20] DOM can also react with ·OH, adding DOM to an aqueous solution containing SCN^- can lead to a decrease in the level of $(SCN)_2^{\cdot-}$ generation. Subsequently, after adding DOM solutions of different concentrations to the system, it was observed that the signal was significantly weakened, indicating that DOM and SCN^- undergo competitive reactions with ·OH, as seen in Fig. 1b. By fitting the $(SCN)_2^{\cdot-}$ signal at different concentrations of DOM, the second-order reaction rate constants of DOM and ·OH were obtained (Fig. 1c). The $k_{DOM,\cdot OH}$ values for three types of DOM samples with ·OH ranged from (3.26 ± 0.72) to (7.38 ± 0.63) × 10^9 M^{-1} s^{-1} (Fig. 1d). The range of $k_{DOM,\cdot OH}$ values reported on an M_C^{-1} s^{-1} basis falls within the range of bimolecular reaction rate constants reported in the literature for oxidizing radicals' reaction with DOM.[5] The high reactivity of DOM to ·OH would affect the efficiency of advanced oxidation processes, decrease the indirect photodegradation of organic pollutants in aquatic environment as well as enhance the formation of disinfection byproducts.[7]

3.2 Impact of ·OH on the molecular properties of DOM

To better understand the changes of DOM induced by the oxidation of ·OH, steady state photochemical experiments were conducted. Firstly, the mineralization process of DOM molecules induced by ·OH was determined using TOC. By analyzing

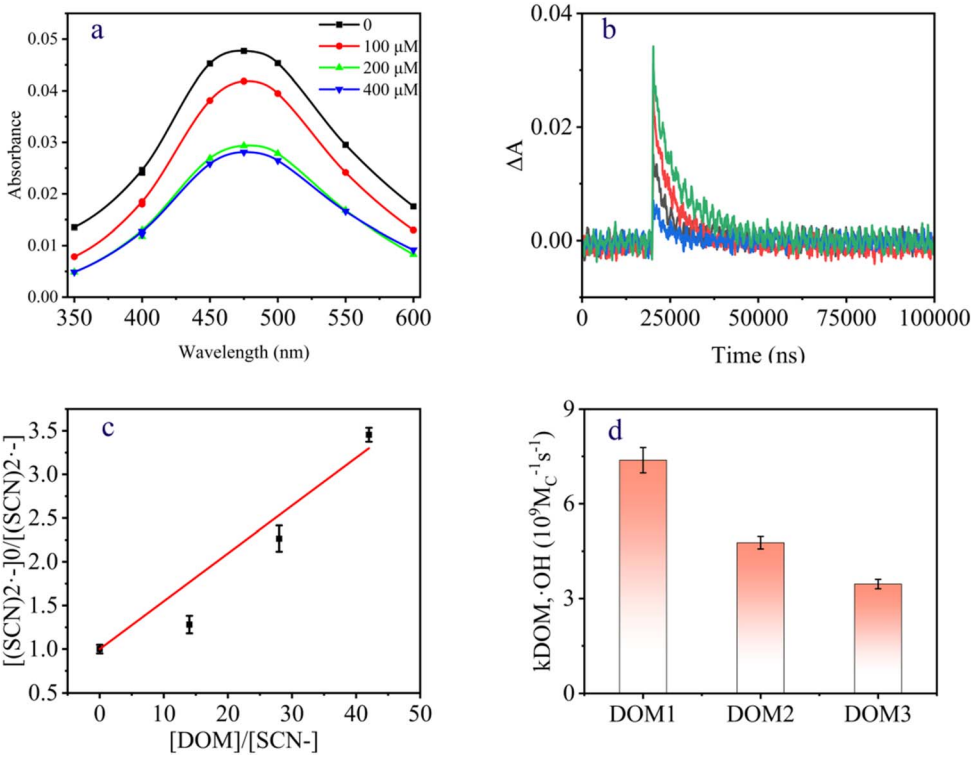

Fig. 1 The second order reaction rate constants between ·OH and three kinds of DOM at pH = 7, room temperature.

the changes in TOC content of each sample in the reaction system, it was found that all three DOM molecules underwent various degrees of mineralization in the presence of sufficient H_2O_2, resulting in a decrease in total organic carbon content; the degradation ratio were up to 79.1%, 72.8, and 44.6% for DOM1, DOM2 and DOM3 respectively (Fig. 2a, c and e). While, the decreases in TOC of the control group (DOM solution without H_2O_2 added) were slight for all three kinds of DOM for the self-sensitized photo-mineralization for the formation of reactive species and direct photodegradation. The results showed that DOM could be mineralized in the presence of $^{\cdot}OH$. We fitted the TOC of DOM solution in the H_2O_2 system over time and found that it did not follow the first-order reaction rate constant (Fig. S4). This indicates that the values of $k_{DOM,^{\cdot}OH}$ are dynamic during the $^{\cdot}OH$ oxidation processes. The easily oxidizable organic moieties (in the surface of DOM macromolecular and electron donating components) was oxidized firstly, which contributed to a fast reactivity to $^{\cdot}OH$, while the residue was refractory to $^{\cdot}OH$ and resulted in a lower $k_{DOM,^{\cdot}OH}$ and lower mineralization rate. The reaction rate between the residue and newly generated refractory organic carbon in the system and $^{\cdot}OH$ will decrease.

In addition, we measured the changes in optical properties of DOM induced by $^{\cdot}OH$. The structure moiety in DOM contributing to the optical properties likely include aromatic carboxylic acids and hydroxy aromatic acids, aromatic ketones and aldehydes, quinones, phenols and polyphenols and N-containing heterocycles. In addition, the absorbance and fluorescent emission processes involve in the charge transfer processes between electron-poor acceptors and electron-rich donors.[21] The changes in optical properties of DOM is a signal for the changes of these functional groups. The UV-visible absorption spectra of the three DOM samples showed varying degrees of photobleaching as the reaction progressed, while the degree of photobleaching was not significant for the blank sample after $^{\cdot}OH$ oxidation, which were consistent with the results of mineralization processes (Fig. 2b, d and f). Due to the absorption of H_2O_2 below 340 nm, in order to avoid

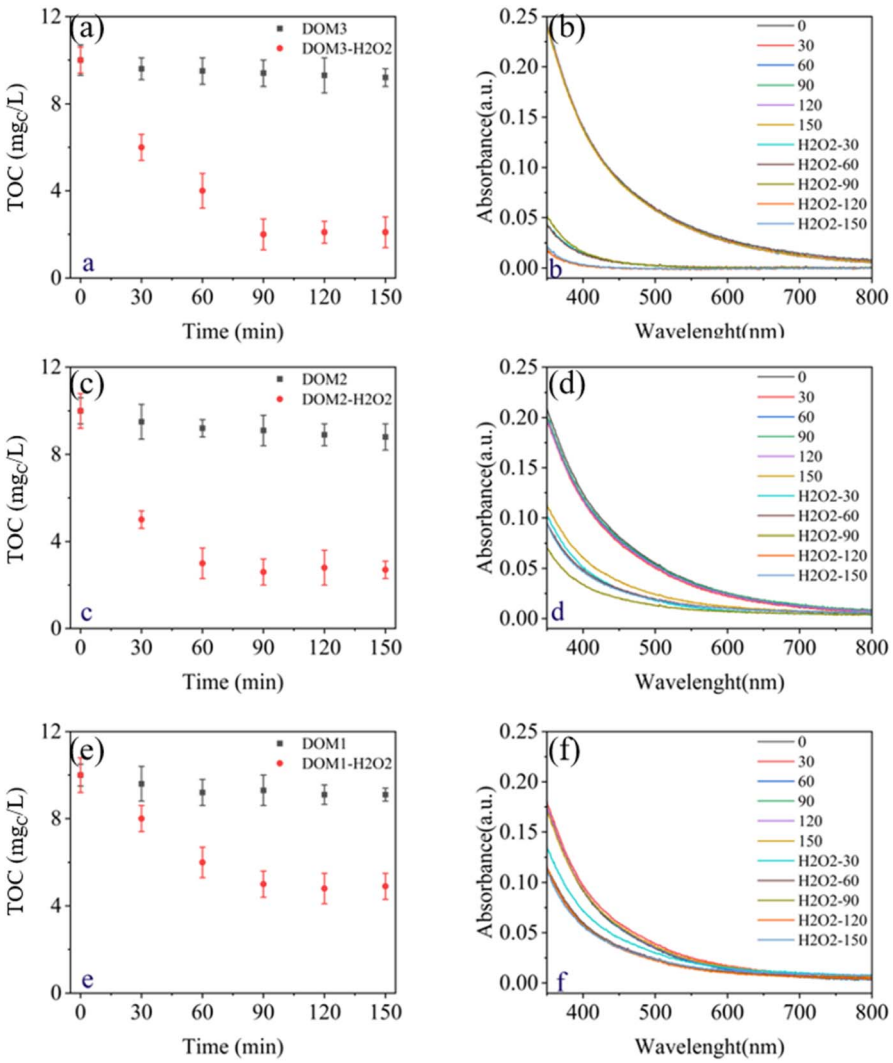

Fig. 2 Changes of TOC (a, c and e) and UV-vis absorbance spectra (b, d and f) of three kinds of DOM in the absence and presence of H_2O_2 ((a and b) for DOM3; (c and d) for DOM2; (e and f) for DOM1).

interference, spectra above 350 nm were selected for investigation. Here, the average of absorbance intensity from 350 to 600 nm (Absave) was used as the absorbance index for DOM, and the absorbance indexes changed during ˙OH oxidation were shown in Fig. S5. Interestingly, there were a sharp bleaching for three kinds of DOM in the presence of H_2O_2 during a 30 min reaction and relative lower bleaching rate after 30 min for all DOM samples. These results indicated that there might some relationship between chromophore moieties and oxidizable organic moieties in DOM (namely phenols, aromatic ketones and quinones *etc.*), which need further investigation.

Fluorescence spectra reflect the fluorescent groups within DOM. By comparing the changes in the 3D-EEM of DOM in the presence and absence of H_2O_2, it was found that the fluorescence peaks of all three types of DOM samples appeared significant red shift, while the changes in the fluorescent groups of DOM samples were not significant in the absence of H_2O_2 (Fig. 3). The results indicate that ˙OH can induce the shift of DOM fluorescent groups, and also suggest that ˙OH may trigger the hydroxylation of DOM molecules, leading to the generation of new fluorescent groups. As the reaction continues, the intensity of the new fluorescent group gradually decreases. The change in fluorescent groups does not result in a significant change in fluorescence intensity during the initial reaction process, but as the reaction progresses, it leads to a decrease in fluorescence intensity, which was different with the monotonically decreasing in chromospheres moieties. The results mean that chromophores and fluorescent moieties were not completely same in DOM. In addition, two fluorescent indexes, namely FI and HIX were calculated to further illustrate the changes of fluorescence moieties in DOM during ˙OH oxidation. In addition, two fluorescence indices, FI and HIX, were calculated to further illustrate changes in fluorescent moieties during ˙OH oxidation. As shown in Fig. S6, HIX decreased for all DOM samples, with a faster decrease in the presence of H_2O_2 than in the corresponding blank groups. In contrast, FI showed an initial increase followed by a decrease for DOM1 and DOM3 in the H_2O_2 system, whereas FI for DOM2 gradually decreased during irradiation times. This behavior indicated that the evolution of fluorescence signatures does not strictly parallel the monotonic bleaching of chromophores, and that the transient formation or transformation of specific fluorophores is sample-dependent.

The oxidation of DOM induced by ˙OH exist in both natural and engineered processes, which played an important role in environmental biogeochemical processes, such as carbon sequestration and cycle. The oxidized residue of DOM had lower fluorescent and chromophore and more refractory than the original DOM, indicating the refractory organic would exist in aquatic environment with a long lifetime. The refractory component should be paid more attention on the effluent organic matter after advanced oxidized processes in engineered

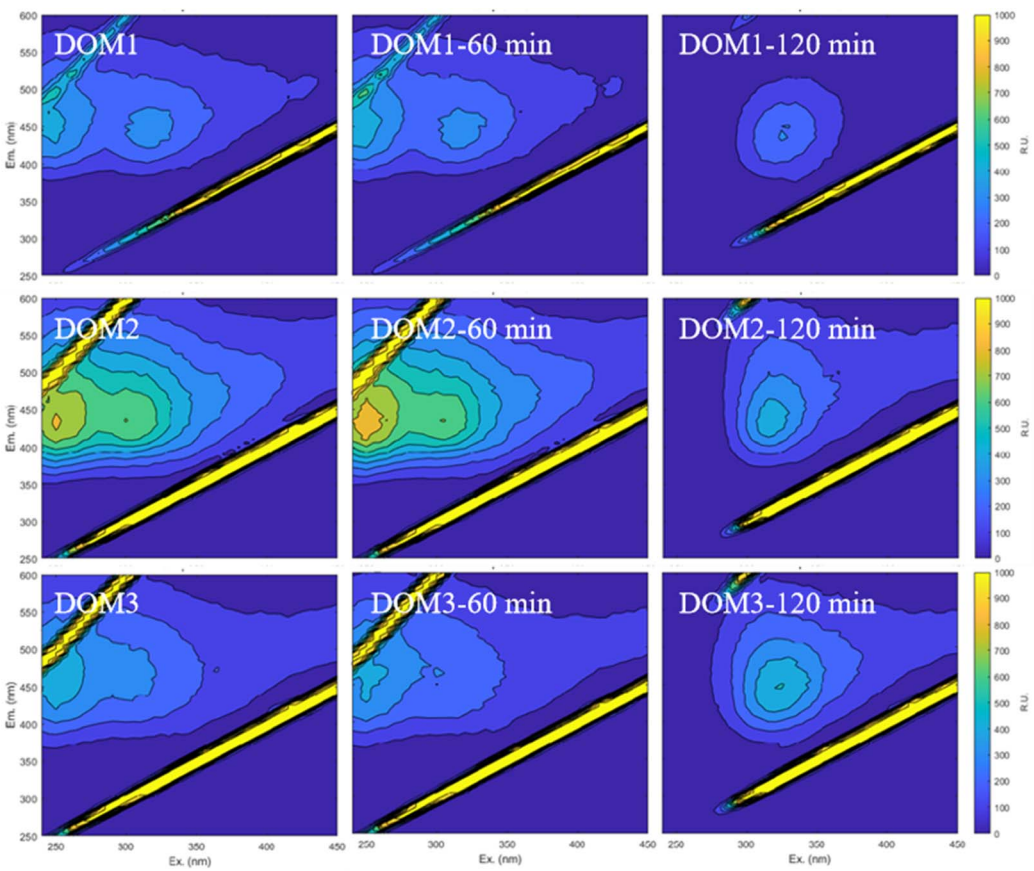

Fig. 3 Changes of 3D-EEMs during the reaction between DOM and ˙OH.

processes and organic matter in natural environment.[22] The environmental behaviors of refractory ble organic matter would not only affect the occurrence, fate and bioavailability of pollutants, but also the biogeochemical cycle of carbon in aquatic environment.[23–28] In addition, the relationship between chromophores, fluorescent moieties, electron-donating moieties and molecular compositions of DOM at molecular level need further investigation.[9,21,29,30]

3.3 Effect of Cu^{2+} on $k_{DOM,\cdot OH}$

DOM is the main sink of ˙OH in natural water, and the quenching reaction could be affected by environmental components. Here, the effects of Cu^{2+} on $k_{DOM,\cdot OH}$ was investigated. For all DOM separated samples, the $k_{DOM,\cdot OH}$ values decreased with increasing Cu^{2+} concentration (Fig. 4 and Table S1), indicating that the presence of Cu^{2+} inhibited the reaction between DOM and ˙OH. In the presence of Cu^{2+}, the $k_{DOM,\cdot OH}$ of three DOM samples decreased, ranging from 60–30%. The decrease in $k_{DOM,\cdot OH}$ indicates that Cu^{2+} inhibits the oxidation of DOM induced by ˙OH. The result was in line with previous study, in which the inhibition effects of Cu^{2+} on the photobleaching of DOM was found.[18] The significant effect of Cu^{2+} indicated that the either water chemistry or environmental properties could also play an important role in the oxidation reaction of DOM induced by ˙OH.

To better understand the effect mechanism of Cu^{2+} on $k_{DOM,\cdot OH}$, the impacts of Cu^{2+} on the molecular properties of DOM were characterized using various spectrum methods. The UV-visible absorbance spectra of three kinds of DOM in the presence of different concentrations of Cu^{2+} were shown in Fig. S7 and the changes of spectra indexes also were summarized in Table S1. The results showed that there was no obvious change in the spectra of UV-vis spectra, while the E2/E3, SR and showed different trends. The changes in SUVA254 mean that the aromatic components in DOM were affected by the interaction between Cu^{2+} and DOM. The decrease of the value of E2 : E3 and increase of SR indicated that the Cu^{2+} could induce the aggregation of DOM samples. The hydrated diameter showed the same trend (Fig. S8 and Table S1). The addition of Cu^{2+} also change the HIX and FI values for all the DOM samples (Table S1). Our previous studies found that the aromatic phenolic groups, aromatic ketones and aromatic carboxylic acids in DOM could bind with Cu^{2+} and form Cu-DOM complexes.[31]

The surface chemistry of DOM, before and after addition of Cu^{2+} was analyzed with XPS. In the C 1 s spectra of DOM, there were three separate peaks at 284.8, 286.5 and 288.3 eV for C–C/C–H, C–O–C and O–C=O respectively. Results indicated a decreasing shift in COO fractions and C–O–C, as well as the increasing move of C–C/C–O after adding of Cu^{2+} (Fig. S9 a–f). The spectral differences implied the complexation between Cu^{2+} and phenol or carboxyl group in DOM. In the Cu 2p spectra, all of the sample showed a split of Cu 2P 3/2, which was attributed to the coexist divalent copper (Cu(II), 933.1 eV) and monovalent cuprous (Cu(I), 932.7 eV) (Fig. S9 g–i). These results suggested that the interaction between Cu^{2+} and DOM could involve in the oxidation and reduction action besides coordination reaction. Previous studies also showed that there were some charge transfer processes during the interaction processes between Cu^{2+} and DOM, and Cu(I) was formed for the charge transfer form ligand to metal (LMCT). Previous studies also found the reduction of Cu^{2+} for the electron donor moiety of DOM.[32] Because Cu(I) has a relatively low oxidation potential, it can in principle be re-oxidized by strong oxidants such as ˙OH, and may participate in redox cycling that influences the net rate of DOM oxidation, thereby contributing to the observed decrease in $k_{DOM,\cdot OH}$.

However, XPS provides only surface-sensitive, semi-quantitative information. The overlap of Cu(I) and Cu(II) peak, the coexistence of multiple Cu species, and matrix effects make accurate Cu speciation and quantification challenging. Consequently, while our XPS data are consistent with partial reduction of Cu(II) to Cu(I) within Cu-DOM complexes, they do not allow us to unambiguously determine the fraction of Cu(I) or its dynamic behavior during ˙OH oxidation. Additional techniques such as XANES/EXAFS, EPR, or electrochemical methods would be required in future work to quantitatively resolve Cu redox speciation and directly verify its kinetic role in DOM oxidation.

The Spearman correlation analysis was conducted to better understand the potential properties influencing the $k_{DOM,\cdot OH}$ values, as shown in Fig. S10. The results showed that $k_{DOM,\cdot OH}$ had a significant positive correlation with E2/E3 and HIX, and a negative correlation with SR and FI. Conventional interpretation is that lower E2 : E3, lower FI are characteristic of DOM with higher molecular weight.[29,30] These results indicated that the molecular weight and diameter played a critical role in the reaction between DOM and ˙OH. The coordination between electron donor moieties and Cu^{2+} and the aggregation of DOM fraction, resulting in inaccessible for ˙OH and the decrease of $k_{DOM,\cdot OH}$. Previous studies have likewise reported that DOM fractions with lower molecular weight tend to exhibit higher $k_{DOM,\cdot OH}$.[13]

Beyond aggregation and site blocking, Pan *et al.* also demonstrated that Cu(I) formed *via* LMCT within Cu-DOM complexes can react as an antioxidant, by reducing phenoxy radicals back to their parent phenols, thereby slowing net DOM oxidation.[18] A similar Cu(I)/Cu(II) redox-shuttle mechanism may also contribute to the decrease in $k_{DOM,\cdot OH}$ in our system.

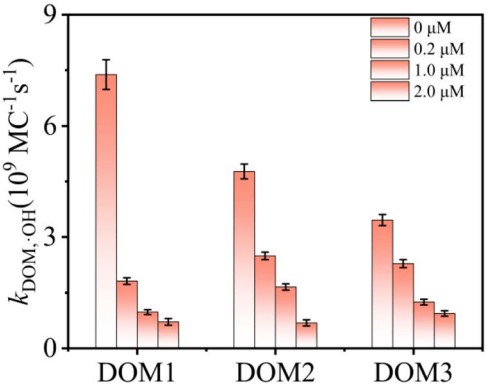

Fig. 4 Bimolecular reaction rate constant measurements between DOM isolates and (˙OH $k_{DOM,\cdot OH}$).

Nonetheless, given the limitations of our current XPS data and the absence of direct measurements of transient radical intermediates, this Cu(I)-mediated protection should be regarded as a plausible, literature-supported auxiliary pathway rather than a fully confirmed dominant mechanism in our study.

In summary, our results indicate that Cu^{2+} reduces $k_{DOM,^{\cdot}OH}$ primarily by promoting DOM aggregation and coordinating with electron-donating functional groups, which together reduce the accessibility and effective reactivity of DOM toward $^{\cdot}OH$. LMCT-induced partial reduction of Cu(II) to Cu(I) and a possible Cu(I)/Cu(II) redox-shuttle effect may further suppress DOM oxidation, although this requires more direct evidence in future work. Moreover, other redox-active metal ions such as Fe and Mn are also expected to modulate DOM–$^{\cdot}OH$ interactions[33] and the influence of broader water constituents on DOM oxidation by photochemically or microbially generated reactive species should be considered in future studies.[8,34]

4. Conclusion

In this study, the reactivity of dissolved organic matter (DOM) toward $^{\cdot}OH$ was quantified, and the influence of Cu^{2+} was systematically evaluated. Using LFP with a competitive kinetics experiment, $k_{DOM,^{\cdot}OH}$ for three DOM samples were determined to range from 3.46 to 7.38 $\times$ 10^9 M^{-1} s^{-1}, confirming that DOM is an $^{\cdot}OH$ scavenger in aquatic systems. Cu^{2+} significantly decreased $k_{DOM,^{\cdot}OH}$ for all DOM samples. The inhibition effect is mainly due to Cu^{2+}-induced aggregation and coordination with electron-donating functional groups, which reduce the accessibility of reactive sites to $^{\cdot}OH$. XPS trends, together with previous studies, further suggest that a Cu(II)/Cu(I) redox "electron-shuttle" associated with DOM–Cu complexes may additionally suppress DOM oxidation, although this mechanism remains tentative and requires more direct verification. Oxidation by $^{\cdot}OH$ induced mineralization, bleaching of chromophores, and quenching or transformation of fluorescent moieties, demonstrating that DOM composition and optical properties are substantially altered during $^{\cdot}OH$ attack. Because DOM efficiently consumes $^{\cdot}OH$, its presence can decrease the effective utilization of $^{\cdot}OH$ in advanced oxidation processes and thus inhibit pollutant degradation. Overall, this work constrains $k_{DOM,^{\cdot}OH}$, elucidates how Cu^{2+} modulates DOM–$^{\cdot}OH$ reactivity *via* changes in DOM molecular properties, and underscores the role of water chemistry in controlling DOM transformation and $^{\cdot}OH$ fate. These findings provide a basis for understanding DOM photo-oxidation in natural waters and for evaluating DOM effects in engineered oxidation systems.

Author contributions

Zhansheng Li: writing – review & editing, writing – original draft, methodology, investigation, conceptualization. Hongxia Zhao: writing – review & editing, validation, supervision, resources, project administration, funding acquisition, conceptualization. Shafiul Azam: writing, review & editing.

Conflicts of interest

The authors declare that they have no known competing financial interests or personal relationships that could have appeared to influence the work reported in this paper.

Data availability

The data supporting this article have been included as part of the supplementary information (SI). Supplementary information is available. See DOI: https://doi.org/10.1039/d5ra09373b.

Acknowledgements

This research was financially supported by the National Key Research and Development Program of China (No. 2022YFC3701404), the National Natural Science Foundation of China (No. 22176025), the National Natural Science Foundation of China (No. 22136007).

References

1 S. E. Page, J. R. Logan, R. M. Cory and K. McNeill, *Environ. Sci.: Processes Impacts*, 2014, **16**, 807–822.
2 G. McKay, *Environ. Sci.: Processes Impacts*, 2020, **22**, 1139–1165.
3 M. Madhiyan and K. J. Moor, *Environ. Sci. Technol.*, 2023, **58**, 1265–1273.
4 J. Peng, Y. Pan, Y. Zhou, X. Lei, Y. Guo, Y. Lei, Q. Kong, S. Cheng and X. Yang, *Environ. Sci. Technol.*, 2024, **58**, 4751–4760.
5 X. Yang, F. L. Rosario-Ortiz, Y. Lei, Y. Pan, X. Lei and P. Westerhoff, *Environ. Sci. Technol.*, 2022, **56**, 11111–11131.
6 G. McKay, M. M. Dong, J. L. Kleinman, S. P. Mezyk and F. L. Rosario-Ortiz, *Environ. Sci. Technol.*, 2011, **45**, 6932–6937.
7 X. Lei, J. Guan, Y. Lei, L. Yao, P. Westerhoff and X. Yang, *Environ. Sci. Technol.*, 2022, **57**, 18597–18606.
8 S. K. Bercovici, M. Wiemers, T. Dittmar and J. Niggemann, *Environ. Sci. Technol.*, 2023, **57**, 21145–21155.
9 M. R. van Erk, O. M. Bourceau, C. Moncada, S. Basu, C. M. Hansel and D. de Beer, *Nat. Commun.*, 2023, **14**, 938.
10 J. Wenk, U. von Gunten and S. Canonica, *Environ. Sci. Technol.*, 2011, **45**, 1334–1340.
11 J. M. Gleason, G. McKay, K. P. Ishida and S. P. Mezyk, *Chemosphere*, 2017, **187**, 123–129.
12 O. S. Keen, G. McKay, S. P. Mezyk, K. G. Linden and F. L. Rosario-Ortiz, *Water Res.*, 2014, **50**, 408–419.
13 G. McKay, J. L. Kleinman, K. M. Johnston, M. M. Dong, F. L. Rosario-Ortiz and S. P. Mezyk, *J. Soils Sediments*, 2013, **14**, 298–304.
14 S. L. Ulliman, G. McKay, F. L. Rosario-Ortiz and K. G. Linden, *Water Res.*, 2018, **130**, 234–242.
15 E. M. White, P. P. Vaughan and R. G. Zepp, *Aquat. Sci.*, 2003, **65**, 402–414.
16 G. McKay, J. A. Korak and F. L. Rosario-Ortiz, *Environ. Sci. Technol.*, 2018, **52**, 9022–9032.

17 M. M. Dong, S. P. Mezyk and F. L. ROSARIO-ORTIZ, *Environ. Sci. Technol.*, 2010, **44**, 5714–5720.
18 Y. Pan, S. Garg, Q.-L. Fu, J. Peng, X. Yang and T. D. Waite, *Environ. Sci. Technol.*, 2023, **57**, 21178–21189.
19 J. Jiang, H. Zhao, S. Liu, X. Chen, X. Jiang, J. Chen and X. Quan, *J. Photochem. Photobiol. A-Chem.*, 2017, **336**, 63–68.
20 M. M. Dong, S. P. Mezyk and F. L. Rosario-Ortiz, *Environ. Sci. Technol.*, 2010, **44**, 5714–5720.
21 G. McKay, *Environ. Sci. Technol. Lett.*, 2021, **8**, 825–831.
22 X. Zheng, R. Cai, H. Yao, X. Zhuo, C. He, Q. Zheng, Q. Shi and N. Jiao, *Environ. Sci. Technol.*, 2022, **56**, 17420–17429.
23 S. Wen, A. Hu, S. Jiang, L. Han, K. S. Jang, A. J. Tanentzap, J. Zhong and J. Wang, *Glob. Change Biol.*, 2024, **30**, e17158.
24 A. Hu, K.-S. Jang, A. J. Tanentzap, W. Zhao, J. T. Lennon, J. Liu, M. Li, J. Stegen, M. Choi, Y. Lu, X. Feng and J. Wang, *Nat. Commun.*, 2024, **15**, 576.
25 Z. Yan, Y. Xin, X. Zhong, Y. Yi, P. Li, Y. Wang, Y. Zhou, Y. Zhou, C. He, Q. Shi and D. He, *Water Res.*, 2023, **244**, 120446.
26 Y. Du, S. An, H. He, S. Wen, P. Xing and H. Duan, *Water Res.*, 2022, **219**, 118560.
27 X. Chen, J. Liu, J. Chen, J. Wang, X. Xiao, C. He, Q. Shi, G. Li and N. Jiao, *Water Res.*, 2022, **220**, 118690.
28 Q. Chen, C. Lønborg, F. Chen, M. Gonsior, Y. Li, R. Cai, C. He, J. Chen, Y. Wang, Q. Shi, N. Jiao and Q. Zheng, *Limnol. Oceanogr.*, 2022, **67**, 2360–2373.
29 J. A. Korak and G. McKay, *Environ. Sci. Technol.*, 2024, **58**, 7380–7392.
30 J. A. Korak and G. McKay, *Environ. Sci.: Processes Impacts*, 2024, **26**, 1663–1702.
31 Z. Li, B. Qu, J. Jiang, T. G. Bekele and H. Zhao, *Sci. Total Environ.*, 2023, 883.
32 G. Xing, S. Garg, C. J. Miller, A. N. Pham and T. D. Waite, *Environ. Sci. Technol.*, 2020, **54**, 2334–2343.
33 O. W. Moore, L. Curti, C. Woulds, J. A. Bradley, P. Babakhani, B. J. W. Mills, W. B. Homoky, K.-Q. Xiao, A. W. Bray, B. J. Fisher, M. Kazemian, B. Kaulich, A. W. Dale and C. L. Peacock, *Nature*, 2023, **621**, 312–317.
34 T. T. H. Nguyen, E. J. Zakem, A. Ebrahimi, J. Schwartzman, T. Caglar, K. Amarnath, U. Alcolombri, F. J. Peaudecerf, T. Hwa, R. Stocker, O. X. Cordero and N. M. Levine, *Nat. Commun.*, 2022, **13**, 1657.